Comparative Study of the Luminescence Properties of the Europium(III) Complexes of the Squarate, Phenylsquarate, and (Diphenylamino)squarate Ligands

Bert D. Alleyne and Lincoln A. Hall*

Department of Chemistry, The University of the West Indies, St. Augustine, Trinidad, West Indies

Ishenkumba A. Kahwa*

Department of Chemistry, The University of the West Indies, Mona, Kingston 7, Jamaica, West Indies

Andrew J. P. White and David J. Williams*

Chemical Crystallography Laboratory, Department of Chemistry, Imperial College of Science, Technology and Medicine, London, SW7 2AY, U.K.

Received June 30, 1999

Reaction of $EuCl_3 \cdot 6H_2O$ with 3-phenyl-4-hydroxycyclobut-3-ene-1,2-dione (phenylsquarate) in methanol produces the polymeric complex $\{Eu(\mu\text{-}C_6H_5C_4O_3)_2(C_6H_5C_4O_3)_2(CH_3OH)_2(H_2O)_2 \cdot (CH_3OH)\}_n$ (**1**) which crystallizes in the space group $P2_1/n$ with $a = 13.4049(5)$ Å, $b = 13.7043(7)$ Å, $c = 18.5026(6)$ Å, $\beta = 106.351(4)°$, and $Z = 4$. The Eu(III) ion is eight coordinate with two bridging and two pendant phenylsquarate ligands, the coordination polyhedron being completed by two aqua and two methanol ligands. The emission spectra of **1** and the already reported europium(III) squarate, $[Eu(H_2O)_4]_2(C_4O_4)_3$ (**2**), and europium(III) (diphenylamino)squarate, $\{Eu[\mu\text{-}(C_6H_5)_2NC_4O_3]_2[(C_6H_5)_2NC_4O_3][NO_3][H_2O]_4\}_2 \cdot 4H_2O$ (**3**) show emissions dominated by the $Eu^{3+}(^5D_0 \rightarrow {}^7F_j)$ transitions which are typical for Eu^{3+} species in low-symmetry sites. For **1** the emission occurs at room temperature and is apparently sensitized by the phenyl substituents on the phenylsquarate ligand groups; for **2** and **3** the emission is only observed at low temperature (77 K). The broad band (370−575 nm) in the excitation spectrum of **3** at 77 K is consistent with excimer formation, which can be attributed to enhanced $\pi-\pi$ interactions between the C_4-cycles of neighboring phenylsquarate ligand groups whose centroid···centroid separation decreases from 3.630(7) Å at room temperature (293 K) to 3.565(7) Å at 96 K. The temperature dependence of the luminescence of all three complexes revealed strong Eu···Eu interactions which keep the energy transport process in the dynamic regime.

Introduction

To assess the effects of monosubstitution of the squarate ligand on, and further understand, the luminescence properties of europium(III) squarate, we decided to study the luminescence spectroscopic properties of the structurally well characterized europium(III) complexes $\{Eu(\mu\text{-}C_6H_5C_4O_3)_2(C_6H_5C_4O_3)_2(CH_3OH)_2(H_2O)_2 \cdot (CH_3OH)\}_n$ (**1**), $[Eu(H_2O)_4]_2(C_4O_4)_3$ (**2**),[1a] and $\{Eu[\mu\text{-}(C_6H_5)_2NC_4O_3]_2[(C_6H_5)_2NC_4O_3][NO_3][H_2O]_4\}_2 \cdot 4H_2O$ (**3**),[1b] which are unequivocally one-dimensional chains, double layers, and dimers, respectively. Apart from the systematic variation in the dimensionality of the Eu(III) cationic array, complexes **1** and **3** were selected since the coordinated monosubstituted squarate ligand in each case demonstrated multiple bond localization, whereas in europium(III) squarate the delocalization extends over the entire squarate ring.[1a] Furthermore, the X-ray structural data suggested that both **1** and **3** had the potential for exhibiting significant $\pi-\pi$ interactions, a feature that was absent in the solid-state structure of **2**.[1] Here we report the synthesis and X-ray structural study of **1** and an analysis of the effects of temperature on the structure of **3** and present a comparative study of the luminescence characteristics of the complexes **1**−**3**.

Experimental Section

Preparation of the Ligand. 1-Phenylcyclobutenedione. 3-Phenyl-4-hydroxycyclobut-3-ene-1,2-dione (phenylsquarate) was prepared according to the method of Liebeskind et al.[2]

Preparation of the Complexes. $\{Eu(\mu\text{-}C_6H_5C_4O_3)_2(C_6H_5C_4O_3)_2(CH_3OH)_2(H_2O)_2 \cdot (CH_3OH)\}_n$ (1). A 20 mL aliquot of a methanolic solution of $EuCl_3 \cdot 6H_2O$ (0.21 g, 5.70×10^{-4} mol) was added to 20 mL of a methanolic solution of phenylsquarate (0.05 g, 1.90×10^{-4} mol). The resulting solution was filtered and left to stand at room temperature in a desiccator until crystallization was complete (yield, 17%).

Anal. Calc for $C_{33}H_{31}EuO_{14}$: C, 49.3; H, 3.9; Eu, 18.9. Found: C, 49.2; H, 3.9; Eu, 17.0 (The sample submitted for Eu analysis may have absorbed water between the polymeric chains on standing, in a manner similar to other phenylsquarate complexes).

$[Eu_2(H_2O)_4]_2(C_4O_4)_3$ (2). A 50 mL aliquot of an aqueous solution of 3-amino-4-methoxycyclobut-3-ene-1,2-dione (0.10 g, 7.90×10^{-4} mol) was mixed with an equal volume of an aqueous solution of

* To whom correspondence should be addressed.

(1) (a) Petit, J.-F.; Gleizes, A.; Trombe, J.-C. *Inorg. Chim. Acta* **1990**, *167*, 51. (b) Alleyne, B. D.; St. Bernard, L.; Jaggernauth, H.; Hall, L. A.; Baxter, I.; White, A. J. P.; Williams, D. J. *Inorg. Chem.* **1999**, *38*, 3774.

(2) Liebeskind, L. S.; Fengl, R. W.; Wirtz, K. R.; Shawe, T. T. *J. Org. Chem.* **1988**, *53*, 2482.

10.1021/ic9907664 CCC: $18.00
Published on Web 12/10/1999

Table 1. Crystallographic Data for **1** and **3a**−**c**

	1	**3a**	**3b**	**3c**
chem formula	$C_{32}H_{27}O_{13}Eu\cdot MeOH$	$C_{64}H_{56}N_6O_{26}Eu_2\cdot 4H_2O$	$C_{64}H_{56}N_6O_{26}Eu_2\cdot 4H_2O$	$C_{64}H_{56}N_6O_{26}Eu_2\cdot 4H_2O$
fw	803.5	1701.1	1701.1	1701.1
space group (No.)	$P2_1/n$ (No. 14)	$P\bar{1}$ (No. 2)	$P\bar{1}$ (No. 2)	$P\bar{1}$ (No.2)
T, K	183	293	203	96
a, Å	13.4049(5)	9.2189(6)	9.2009(3)	9.1891(4)
b, Å	13.7043(7)	9.8147(7)	9.7464(11)	9.6966(4)
c, Å	18.5026(6)	19.0860(8)	19.0556(6)	19.0240(8)
α, deg		78.472(4)	78.049(6)	77.630(3)
β, deg	106.351(4)	82.386(7)	82.330(3)	82.293(3)
γ, deg		88.340(3)	88.012(5)	87.787(3)
V, Å^3	3261.5(2)	1677.2(2)	1656.8(2)	1640.70(12)
Z	4	1 [a]	1 [a]	1 [a]
ρ_{calcd}, g cm^{-3}	1.636	1.684	1.705	1.722
λ, Å	1.541 78	0.710 73	1.541 78	0.710 73
μ, cm^{-1}	143.8	19.5	142.4	19.9
R_1 [b]	0.056	0.047	0.055	0.043
wR_2 [c]	0.151	0.095	0.141	0.103

[a] The complex has crystallographic C_i symmetry. [b] $R_1 = \sum||F_o| - |F_c||/\sum|F_o|$. [c] $wR_2 = \{\sum[w(F_o^2 - F_c^2)^2]/\sum[w(F_o^2)^2]\}^{1/2}$. $w^{-1} = \sigma^2(F_o^2) + (aP)^2 + bP$.

$Eu(NO_3)_3\cdot 5H_2O$ (0.34 g, 7.90×10^{-4} mol). The mixture was then filtered and the filtrate allowed to evaporate slowly at room temperature (ca. 28 °C) until crystallization was complete. (Note: 3-Amino-4-methoxycyclobut-3-ene-1,2-dione instead of squaric acid was used in the preparation of the complex because we were aware that both the amino and methoxy groups hydrolyzed during the synthesis to produce better quality crystals of **2**.)

$\{Eu[\mu\text{-}(C_6H_5)_2NC_4O_3]_2[(C_6H_5)_2NC_4O_3][NO_3][H_2O]_4\}_2\cdot 4H_2O$ (3). This complex was prepared according to the method of Alleyne et al.[1b]

Preparation of Mixed Metal Complexes. All mixed metal complexes were prepared using procedures similar to those for their pure counterparts with the appropriate metal ratios. The results of the actual metal analyses done on the mixed metal complexes were used in calculating the molecular formulas presented in the discussion. For example, analysis of the mixed gadolinium(III)/europium(III) squarate complex gave 28.8% Gd and 0.7% Eu, which correspond approximately to $[Gd_{0.98}Eu_{0.02}(H_2O)_4]_2(C_4O_4)_3$.

Elemental Analyses. C, H, N, and metal analyses were performed by MEDAC Ltd., Brunel Science Centre, Egham, Surrey, U.K.

Spectroscopy. The emission and excitation spectra were recorded using an LS-5B Perkin-Elmer fluorescence spectrometer (accuracy = ±2 nm, repeatability = ±1 nm, and resolution = 2 nm for a 10 nm slit width; signal:noise ≥ 70:1) in the phosphorescence mode. The spectrometer was interfaced to a computer via a program written by Dr. Robertha C. Howell.

Luminescence Decay Kinetics. The luminescence decay rates were measured using a pulsed Photon Technology International (PTI) PL 2300 nitrogen laser, which pumps a PL201 dye laser. The laser has a pulse width of 1 ns and a maximum energy of 1.4 mJ per pulse. The emission was detected by a Hamamatsu R928 photomultiplier tube and passed through an NE 531N preamplifier. This was then sampled by a Tektronics 2232 oscilloscope (100 mHz bandwidth, 100 megasamples/s, 1000 channels, 8 bit digitizer, and 16 bit storage amplitude resolution). Approximately 1024 transients were averaged by the oscilloscope, transferred to a 486 PC for further averaging and analysis using a nonlinear Marquardt procedure. For 77 K measurements, the samples were sealed in 4 mm thick glass tubes and placed in a finger type quartz EPR dewar. Variable temperature analyses (10−320 K) were done using an APD Cryogenics Inc. CSW-202 Displex helium refrigerator system. Direct excitation of the $^5D_0$ state was at 580 nm, and emission was monitored at 610 nm. Indiscriminate excitation was at 337 nm.

Crystallography. Table 1 provides a summary of the crystallographic data for compounds **1** and **3a**−**c**. For **1** and **3b** data were collected on a Siemens P4/RA diffractometer using graphite monochromated Cu Kα radiation, while for **3a** and **3c** the data were collected on a Siemens SMART CCD diffractometer using graphite monochromated Mo Kα radiation. In each case the data were corrected for Lorentz and polarization factors, and for absorption. The structures were solved by direct methods, and the non-hydrogen atoms were refined anisotropically using full matrix least-squares based on F^2 (the pendant phenyl rings were refined as idealized rigid bodies). In all four structures the C−H hydrogen atoms were placed in calculated positions, assigned isotropic thermal parameters, $U(H) = 1.2U_{eq}(C)$ [$U(H) = 1.5U_{eq}$(C−Me)], and allowed to ride on their parent atoms. Though in **1** the O−H hydrogen atoms could not be located, in **3a**−**c** they were located from ΔF maps, assigned isotropic thermal parameters, $U(H) = 1.2U_{eq}(O)$, and refined subject to an O−H distance constraint (0.90 Å). All computations were carried out using the SHELXTL PC program system.[3] Crystallographic data are available from the Cambridge Crystallographic Database; use reference numbers CCDC 137562 (**1**), 137564 (**3a**), 132371 (**3b**), and 137563 (**3c**).

Results and Discussion

Structure of $\{Eu(\mu\text{-}C_6H_5C_4O_3)_2(C_6H_5C_4O_3)_2(CH_3OH)_2(H_2O)_2\cdot(CH_3OH)\}_n$ (1). The X-ray analysis of the complex formed between the phenylsquarate ligand and $EuCl_3\cdot 6H_2O$ shows the europium to be bonded to four phenylsquarate groups, two methanols, and two water molecules (Figure 1). Two of the phenylsquarate units are monodentate, while the third (which is related to the fourth by symmetry) is 1,3-binucleating, linking adjacent europium centers to form a polymer chain that propagates via the crystallographic 2_1 screw (Figure 2). The geometry at europium is slightly distorted square antiprismatic, the top and bottom faces being parallel to within 2° and staggered by ca. 38° with respect to each other (Figure 3). The Eu−O distances are in the range 2.348(6)−2.453(7) Å, the shortest contacts being to the phenylsquarate ligands. It is interesting to note that there is a marked asymmetry in the coordination distances to the binucleating phenylsquarate ligands—2.348(6) [O(1)] and 2.402(6) Å [O(3A)]—though there is no significant difference in the associated C═O distances. The Eu−O−C(phenylsquarate) angles are in the range 134.0(6) [O(3)] to 150.0(6)° [O(11)] (Table 2). The phenyl substituent is oriented cis with respect to the ligating oxygen in both the pendant and μ-1,3-bridging phenylsquarate ligand groups.

A pronounced conformational feature of all three independent phenylsquarate ligands is a near-coplanar relationship between their C_4 and phenyl rings, the torsional twists about the bond linking the two ring systems being 7, 2, and 2° for the C(1), C(11), and C(21) containing ligands, respectively. This geometry favors conjugation between the two ring systems and is

(3) *SHELXTL PC version 5.03*; Siemens Analytical X-ray Instruments, Inc.: Madison, WI, 1994.

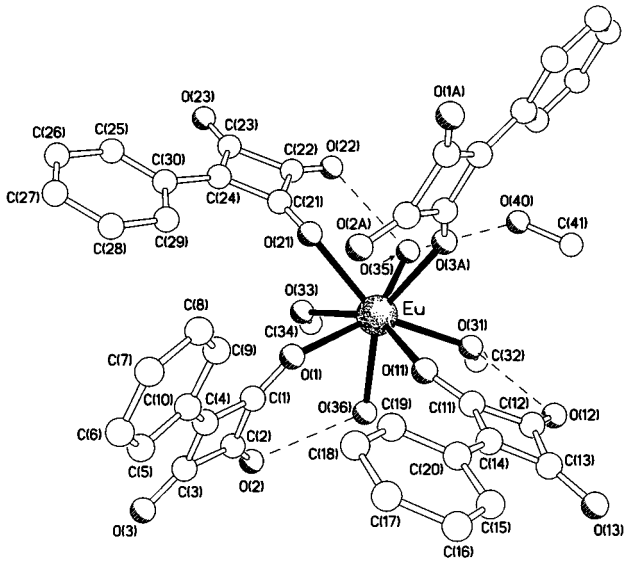

Figure 1. Coordination environment of the europium center in the structure of **1** showing also the intramolecular O−H···O hydrogen bonds and the linking to the included methanol solvent molecule. (The phenylsquarate ligand coordinated through O(3A) is related by symmetry to that coordinated through O(1)).

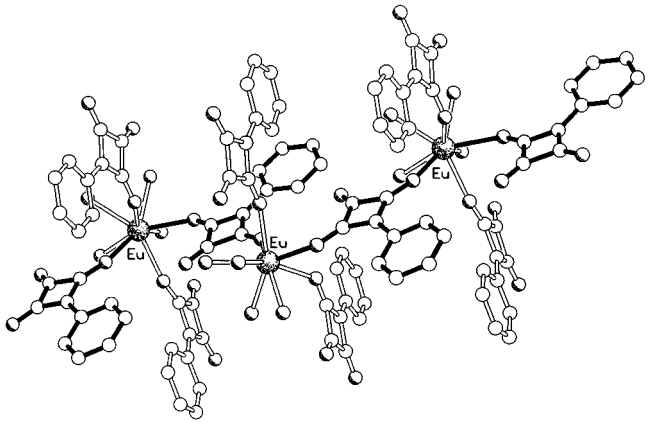

Figure 2. Part of one of the 2_1 screw propagated polymer chains in the structure of **1**. The Eu···Eu separations are 8.27 Å (the methanol methyl groups have been omitted for clarity).

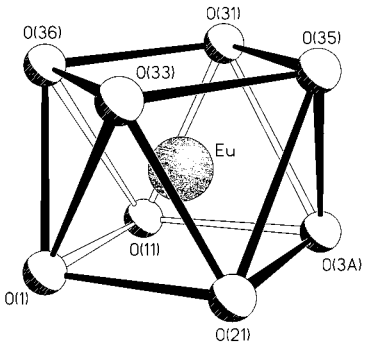

Figure 3. Square antiprismatic europium coordination polyhedron present in the crystals of **1**.

accompanied by a shortening of the inter-ring bond lengths which range between 1.451(10) and 1.454(10) Å (compared with, for example, a mean inter-ring distance of ca. 1.49 Å in biphenylene containing compounds). The pattern of bonding within all three independent C_4-ring systems are, despite the inevitably large estimated standard deviations (esd's), remarkably consistent, with the two bonds adjacent to the phenyl substituent (average 1.443 Å) being shorter than the others (average 1.518 Å). Thus, the multiple bond localization observed in all the transition metal and lanthanide complexes of monosubstituted squarate ligands reported so far is also observed in this complex.[1b,4] Furthermore, the magnitude of Δ(C−C) does not differ significantly for the first row transition methylsquarates, phenylsquarates, or **1**, thus providing further evidence that the magnitude of Δ(C−C) is solely dependent on the identity of the substituent.[4]

Adjacent polymer chains are aligned parallel, the monodentate phenylsquarate ligands in one chain intercalating between their counterparts in the next forming ···ABBAAB··· stacks where A and B are the two independent monodentate ligands (Figure 4). Ligands of "like" type (i.e. AA or BB) are aligned in an overlapping, head-to-tail, C_i symmetric arrangement with mean interplanar separations of 3.35 and 3.51 Å, respectively, while

Table 2. Selected Bond Lengths (Å) and Angles (deg) for $\{Eu(\mu\text{-}C_6H_5C_4O_3)_2(C_6H_5C_4O_3)_2(CH_3OH)_2(H_2O)_2\cdot(CH_3OH)\}_n$ (**1**)

Eu−O(1)	2.348(6)	Eu−O(31)	2.453(7)
Eu−O(3)#1	2.402(6)	Eu−O(33)	2.459(6)
Eu−O(11)	2.350(6)	Eu−O(35)	2.415(5)
Eu−O(21)	2.386(6)	Eu−O(36)	2.444(6)
O(1)−C(1)	1.234(11)	O(21)−C(21)	1.220(10)
O(2)−C(2)	1.213(11)	O(22)−C(22)	1.200(12)
O(3)−C(3)	1.239(11)	O(23)−C(23)	1.197(11)
O(11)−C(11)	1.260(12)	O(31)−C(32)	1.435(11)
O(12)−C(12)	1.220(12)	O(33)−C(34)	1.441(11)
O(13)−C(13)	1.223(11)	O(40)−C(41)	1.393(14)
C(1)−C(2)	1.522(12)	C(11)−C(12)	1.503(13)
C(2)−C(3)	1.506(12)	C(12)−C(13)	1.515(12)
C(3)−C(4)	1.437(12)	C(13)−C(14)	1.444(13)
C(1)−C(4)	1.435(12)	C(11)−C(14)	1.418(12)
C(4)−C(10)	1.454(10)	C(14)−C(20)	1.451(10)
O(1)−Eu−O(11)	75.8(2)	O(11)−Eu−O(21)	117.5(2)
O(11)−Eu−O(3)#1	75.0(2)	O(1)−Eu−O(35)	146.5(2)
O(21)−Eu−O(35)	83.3(2)	O(21)−Eu−O(36)	135.4(2)
O(1)−Eu−O(36)	76.6(2)	O(35)−Eu−O(36)	108.2(2)
C(11)−O(11)−Eu	150.0(6)	C(32)−O(31)−Eu	126.1(6)

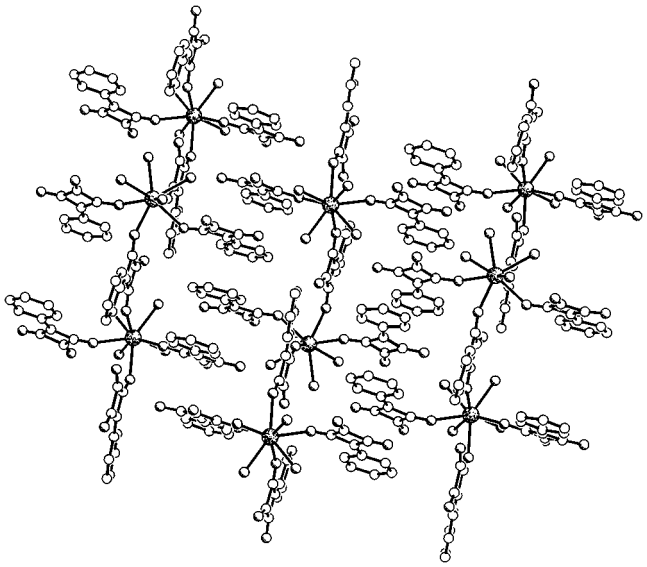

Figure 4. π-stacking of adjacent polymer chains in the structure of **1** (the methanol methyl groups have been omitted for clarity).

(4) (a) Alleyne, B. D.; Hosein, H.-A.; Jaggernauth, H.; Hall, L. A.; White, A. J. P.; Williams, D. J. *Inorg. Chem.* **1999**, *38*, 2416. (b) Hosein, H.-A.; Jaggernauth, H.; Alleyne, B. D.; Hall, L. A.; White, A. J. P.; Williams, D. J. *Inorg. Chem.*, in press. (c) Alleyne, B. D.; Williams, A.; Hosein, H.-A.; Jaggernauth, H.; Hall, L. A.; Foxman, B. *Inorg. Chem.*, submitted for publication.

AB and BA pairs are oriented head-to-head and tail-to-tail with a mean interplanar separation of 3.36 Å, the ring systems being inclined by only ca. 4° to each other. These $\pi-\pi$ interactions serve to cement adjacent polymer chains to form sheets and are supplemented by a pair of strong intermolecular O−H···O hydrogen bonds between (i) the methanol oxygen O(33) in one chain and the carbonyl oxygen O(13) in the next (2.62 Å) and (ii) one of the aqua oxygens [O(36)] in one chain and the carbonyl oxygen O(23) in the next (2.64 Å). [Although the methanol and aqua hydrogen atoms could not be located, an analysis of the spacial relationships of the proximal potential donors and acceptors indicated an unambiguous pattern for the hydrogen bonding interactions.] The other coordinated donors are involved in intrachain O−H···O hydrogen bonds, with the methanol oxygen O(31) being linked to the carbonyl oxygen O(12) (2.76 Å) and the aqua oxygens O(35) and O(36) linking to the carbonyl oxygens O(22) and O(2) at 2.73 and 2.79 Å, respectively. The structure contains an ordered methanol solvent molecule [O(40)−C(41) in Figure 1], which is hydrogen bonded to the aqua oxygen O(35) at 2.67 Å, and also cross-links adjacent $\pi-\pi$ stacked/hydrogen bonded sheets via a further hydrogen bond to the carbonyl oxygen O(22) (2.73 Å).

Complexes **1**−**3** offer an interesting series of structural motifs for investigating the influence of the dimensionality of the Eu(III) array on the luminescence spectroscopic and energy transport behavior.[5,6] In particular, the luminescence characteristics of $[\{Eu_2(H_2O)_4\}_2(C_4O_4)_3]_n$ at room temperature and 4 K were recently described by Donega et al.[7a,b] and Legendziewicz[7c] and indicated severe temperature dependence, but no systematic variable temperature studies were performed. We thus sought to study the comparative temperature evolution of the Eu^{3+} in the $[Eu(H_2O)_4]_2(C_4O_4)_3$ layers, $\{Eu(\mu\text{-}C_6H_5C_4O_3)_2(C_6H_5C_4O_3)_2(CH_3OH)_2(H_2O)_2\cdot(CH_3OH)\}_n$ chains, and $\{Eu[\mu\text{-}(C_6H_5)_2NC_4O_3]_2[(C_6H_5)_2NC_4O_3][NO_3][H_2O]_4\}_2\cdot 4H_2O$ dimers in order to establish the factors responsible for the severe temperature dependence of $[\{Eu_2(H_2O)_4\}_2(C_4O_4)_3]_n$ and the influence of the dimensionality of the Eu(III) ion array on the energy transport regime.

Luminescence Spectroscopy. In sharp contrast to the crystalline europium(III) squarate (coordination site symmetry ca. D_{4d}), the compound europium(III) phenylsquarate (also coordination site symmetry ca. D_{4d}) luminesces at room temperature (albeit weakly) and exhibits a strong red emission at 77 K (Figure 5). For Eu(III) at a strictly D_{4d} site, the $Eu^{3+}(^5D_0\rightarrow{}^7F_j)$ (j = 0, 2, 3) transitions are forbidden.[5] However, for both **1** (Figure 5) and **2** (Figure 4, ref 7b) the so-called hypersensitive Eu^{3+}-$(^5D_0\rightarrow{}^7F_2)$ transition dominates the emission spectra. For both **1** and **2** the strictly forbidden $Eu^{3+}(^5D_0\rightarrow{}^7F_0)$ transition is also noticeable; this is usually symptomatic of Eu^{3+} at a site of low symmetry (C_{2v} or less).[5] While the arrangement of oxygen atoms around Eu(III) ions in both **1** and **2** is close to D_{4d}, the effective symmetry of the crystal electric field at those Eu(III) ions may be different. For example for **2**, the individual contributions of the two water and two methanol molecules as well as two terminal (involved in extended π-π interactions) and two bridging phenylsquarate anions could differ markedly, thereby generating a net crystal field of much lower symmetry than D_{4d} at the Eu(III) center. While this might explain the significant intensities of the $Eu^{3+}(^5D_0\rightarrow{}^7F_j$ [j = 0,2]) transitions, it does not persuasively account for the very low intensity of, what should then be, an allowed $Eu^{3+}(^5D_0\rightarrow{}^7F_4)$ transition (Figure 5). Once again, the electronic behavior of Eu(III) in 'D_{4d} coordination sites' is enigmatic.[5,7] Perhaps detailed theoretical analyses of ligand polarization effects on various crystal field components of the Eu^{3+} ^7F_j levels (including quadrupolar effects) might be helpful.[5f]

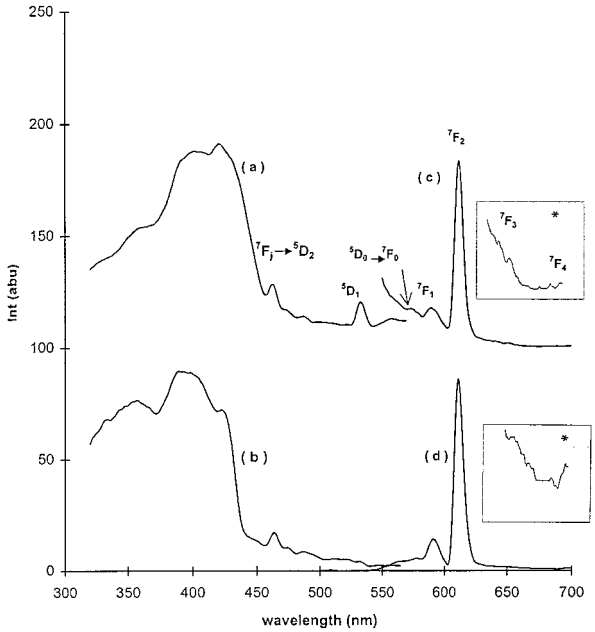

Figure 5. Emission and excitation spectra of europium(III) phenylsquarate at room temperature (rt) and 77 K: (a) the excitation spectrum at rt (λ_{em} = 610 nm, t_g = 0.01, t_d = 0.01); (b) the excitation spectrum at 77 K (λ_{em} = 610 nm, t_g = 0.01, t_d = 0.01); (c) the emission spectrum at rt (λ_{exc} = 360 nm, t_g = 0.01, t_d = 0.01); (d) the emission spectrum at 77 K (λ_{exc} = 360 nm, t_g = 0.01, t_d = 0.01). Insert (∗): Expansion of 620−700 nm region.

Besides the europium(III) transitions, the emission spectrum of **1** at room temperature (Figure 5c) features a broad emission at lower wavelengths that is due to overlapping squarate ring[7a,b] and phenyl moiety electronic transitions. The emission at 77 K is similar except for the disappearance of squarate emission and relatively greater prominence of the broad underlying feature (550−700 nm) (Figure 5d) due to the phenyl moiety, which is in good spectral overlap with $Eu^{3+}(^5D_{J'}\leftarrow{}^7F_J$ [J' = 0,1]) absorptions. For this reason, the phenyl substituents are better sensitizers for $Eu^{3+}(^5D_0\rightarrow{}^7F_2)$ emission than the squarate ring, even though the latter is in direct contact with the Eu^{3+} ion. Thus at room temperature the excitation spectrum of Eu^{3+}-$(^5D_0\rightarrow{}^7F_2)$ emission is dominated by a poorly resolved absorption envelope centered at 400 nm; sharp $Eu^{3+}(^5D_{J'}\leftarrow{}^7F_J)$ absorptions, including the hot band system $Eu^{3+}(^5D_{J'}\leftarrow{}^7F_1)$ due to Boltzman population of low-lying $^7F_1$, are also present. At low wavelengths, absorptions typical of the squarate moiety (as observed in the excitation spectrum of **2**)[7a,b] appear as weak shoulders at wavelengths < 350 nm. At 77 K both the characteristic squarate (at ca. 350 nm) and the phenyl (at ca. 400 nm) absorptions are strong, but the latter is narrower compared to the corresponding transition at room temperature, and the hot band at ca. 533 nm is not observed. Thus in europium phenylsquarate the ligand efficiently sensitizes Eu^{3+}-

(5) (a) Gajadhar-Plummer, A. S.; Kahwa, I. A.; White, A. J. P.; Williams, D. J. *Inorg. Chem.* **1999**, *38*, 1745. (b) Blasse, G. *Inorg. Chim. Acta* **1988**, *142*, 153. (c) Thompson, L. C.; Kuo, S. C. *Inorg. Chim. Acta* **1988**, *149*, 305. (d) Sinha S. P.; Butter, E. *Mol. Phys.* **1969**, *16*, 285. (e) Försberg, J. H. *Coord. Chem., Rev.* **1973**, *10*, 195. (f) Mason, S. F.; Peacock, R. D.; Stewart, B. *Chem. Phys. Lett.* **1974**, *29*, 149.

(6) Kahwa, I. A.; Parkes, C. C.; McPherson, G. L. *Phys. Rev.* **1995**, *B52*, 1177.

(7) (a) Ribeiro, S. J. L.; Goncalves, R. R.; de Oliveira, L. F. C.; Santos, P. S. *J. Alloys Compd.* **1994**, *216*, 61. (b) Donega, C. de M.; Ribeiro, S. J. L.; Goncalves, R. R.; Blasse, G. *J. Phys. Chem. Solids* **1996**, *57*, 1727. (c) Legendziewicz, J. *Acta Phys. Pol. A* **1996**, *90*, 127.

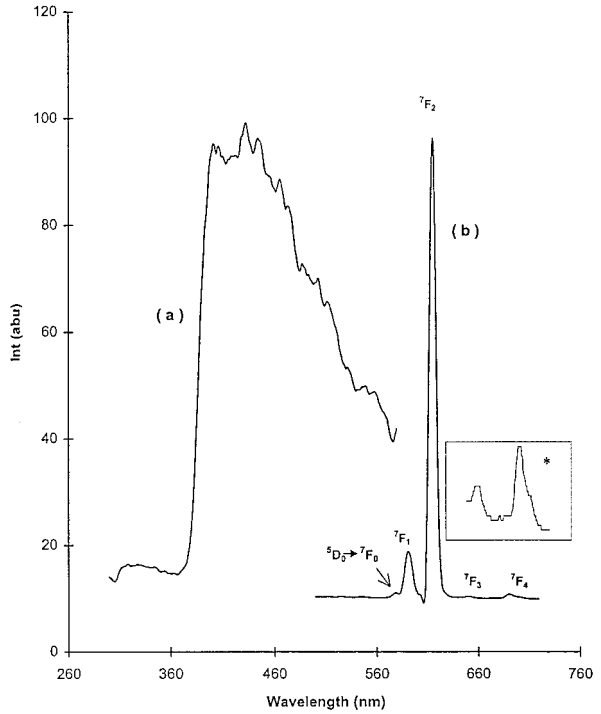

Figure 6. Emission and excitation spectra of europium(III) (diphenylamino)squarate (**3**) at 77 K: (a) the excitation spectrum with λ_{em} = 610 nm, $t_g = 0.01$, and $t_d = 0.1$; (b) the emission spectrum with λ_{exc} = 520 nm, t_g m= 0.05, and $t_d = 0.05$. Insert (*): Expansion of 620−700 nm region.

($^5D_0 \rightarrow ^7F_j$) emission because of direct ligand−Eu interaction due to extended delocalization involving the π-orbitals of the phenyl substituents and C_4-rings via conjugation as evidenced by the short $C_{phenyl}-C_4$ bonds. It was therefore interesting to study the luminescence characteristics of europium (diphenylamino)squarate (**3**) in which significant interaction between the nitrogen lone pair of the diphenylamino substituent and the C_4-ring is also evident from the short $N-C_4$ bond length [1.37(9) Å] compared to the $N-C_{phenyl}$ bond [1.42(1) Å].[1a]

The emission spectrum (λ_{exc} = 360 nm) (Figure 6b) of europium (diphenylamino)squarate (**3**) at 77 K is dominated by the $Eu^{3+}(^5D_0 \rightarrow ^7F_2)$ transition. $Eu^{3+}(^5D_0 \rightarrow ^7F_j[j=0,1,4])$ transitions are also observed which is consistent with Eu^{3+} being at the low-symmetry site (distorted monocapped square antiprism which, additionally, is derived from different types of oxygen atoms [Figure 2, ref 1b]). No emission is observed at room temperature. With smaller delay and gating times the Eu^{3+}-($^5D_1 \rightarrow ^7F_j$) and a broad weak underlying emission are also found. The excitation spectrum (λ_{em} = 610 nm) features a very broad asymmetric absorption band ($\lambda > 370$ nm) (Figure 6a); no sharp europium bands are observed. The squarate absorptions centered at ca. 330 nm are very weak, which shows that the intense broad absorption ($\lambda > 370$ nm) due to electronic transitions within the extensively delocalized (diphenylamino)squarate ligand are good sensitizers for $Eu^{3+}(^5D_0 \rightarrow ^7F_j)$ emission. This broad absorption results in a low-energy broad emission (at ca. 540−700 nm), which overlaps well with the Eu(III) absorptions, especially the $Eu^{3+}(^5D_0 \leftarrow ^7F_J)$. The electron delocalization, involving largely the lone pair on the nitrogen atom (the pyramidalization on the nitrogen site is very small) and the C_4-cycle, was described in detail previously.[1b] While the broad absorption commences in the same general region (at ca. 370 nm) as the phenyl absorption of the phenylsquarate complex, the spectral profile (Figure 6a) seems roughly similar to those generally exhibited by exciplex and excimeric states.[8] Excimer/exciplex formation may be favored by the enhanced potential of $\pi-\pi$ interaction arising from the reduced separation of the C_4-cycles of neighboring (diphenylamino)squarate ligand groups [i.e. 3.630(7), 3.591(7), and 3.565(7) Å at 293, 203, and 96 K, respectively]. Compared to the contribution of the (C_4-cycle)-to-europium(III) energy transfer (Figure 6), the extended electronic interactions between the diphenylamino substituent and the C_4-ring along with the concomitant exciplex/excimer-type states are more efficient sensitizers of $Eu^{3+}(^5D_0 \rightarrow ^7F_j)$ emission. To better understand these processes and the remarkable temperature dependence of the $Eu^{3+}(^5D_0 \rightarrow ^7F_j)$ emission, we undertook a comparative study of the temperature evolution of the luminescence decay behavior of **1**−**3**.

Luminescence Decay Dynamics of $Eu^{3+}(^5D_0)$ Emission in Crystalline Double Layers of $[Eu_2(H_2O)_4]_2(C_4O_4)_3$ (2). The luminescence decay curves of $[Ln(H_2O)_4]_2(C_4O_4)_3$ are severely temperature dependent. Indiscriminate excitation of the $[Gd_{0.98}Eu_{0.02}(H_2O)_4]_2(C_4O_4)_3$ complex at $T < 233$ K leads to perfect single-exponential decay behavior, following an excitation build up (e.g. ca. 2.8×10^5 s^{-1} at 77 K); thereafter marginal deviations from single-exponential behavior are observed. Following direct excitation of the $^5D_0$ level, the pure europium complex **2** features perfect single-exponential behavior for $T < 243$ K; thereafter the emission is weak and deviates marginally from single-exponential decay behavior. At 77 K and indiscriminate excitation at 337 nm, the decay curve for **2** features an excitation build up of ca.4.8×10^5 s^{-1} which corresponds to the decay rate of the $Eu^{3+}(^5D_1 \rightarrow ^7F_j)$ emission of ca.4.8×10^5 s^{-1}. This means that ligand-to-europium energy transfer in these compounds is very fast relative to internal conversions from upper states to $Eu^{3+}(^5D_0)$. In both $[Gd_{0.98}Eu_{0.02}(H_2O)_4]_2(C_4O_4)_3$ and **2** the spontaneous decay rate is ca. 7.0×10^3 s^{-1}. However, the temperature-dependent decay rates of the $^5D_0$ emission in the dilute compound $[Gd_{0.98}Eu_{0.02}(H_2O)_4]_2(C_4O_4)_3$ are marginally but systematically lower than those of the pure europium compound **2**. This indicates that at low temperature energy migration in crystals of the pure two-dimensional europium compound **2** is active but traps for europium(III) excitation are under these conditions not efficient enough to significantly quench the metal emission. An Arrhenius plot utilizing europium(III) $^5D_0$ emission decay rates derived from temperature-dependent single-exponential decay curves reveals the thermal barriers of ca. 3.2×10^3 cm^{-1} mol^{-1} for $[Gd_{0.98}Eu_{0.02}(H_2O)_4]_2(C_4O_4)_3$ (at $77 < T < 273$ K), 1.4×10^3 cm^{-1} mol^{-1} for **2** (at $203 < T < 243$ K), and 3.3×10^3 cm^{-1} mol^{-1} for **2** (at $243 < T < 263$ K). The biphasic temperature dependence of the concentrated **2** complex was confirmed by a study of its more luminescent, deuterated derivative, $[Ln(D_2O)_4]_2(C_4O_4)_3$, for which the thermal barriers are ca. 8.4×10^2 ($193 < T < 223$ K) and 3.2×10^3 ($233 < T < 263$ K) cm^{-1} mol^{-1}. The large difference between the thermal barriers of the dilute Eu/Gd and concentrated hydrate **2** and its deuterated derivative indicates significant differences in $Eu^{3+}(^5D_0 \rightarrow ^7F_j)$ luminescence quenching mechanisms. For the dilute $[Gd_{0.98}Eu_{0.02}(H_2O)_4]_2(C_4O_4)_3$ compound energy migration on the europium(III) sublattice is inefficient, and therefore a higher thermal barrier is required to bridge the emitting $Eu^{3+}(^5D_0)$ state with that of some (unidentified) higher energy (20 500 cm^{-1}) trapping state. The most significant luminescence-quenching pathway for **2** requires fast energy migration on the $Eu^{3+}(^5D_0)$ sites followed by phonon-assisted energy transfer to thermally accessible traps (for $T <$ 243 K). Above 243 K, the luminescence decay kinetics of **2**

(8) Winnik, F. M. *Chem. Rev.* **1993**, *93*, *587*.

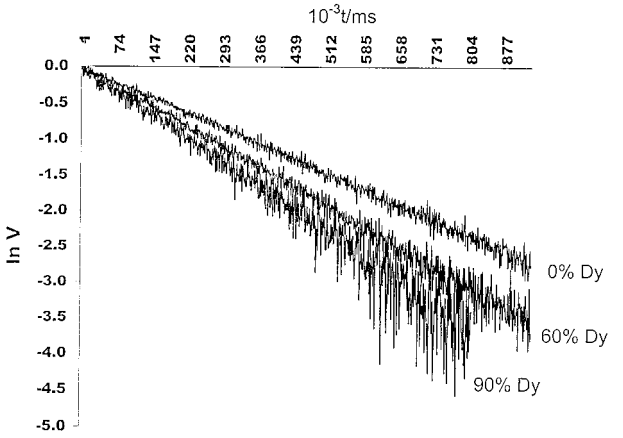

Figure 7. Dependency of the 297 K luminescence decay curves of $Eu^{3+}(^5D_0)$ (emission, 610 nm; excitation, 580 nm) on the concentration of Dy^{3+} quenchers in $\{Eu_{1-x}Dy_x(\mu\text{-}C_6H_5C_4O_3)_2(C_6H_5C_4O_3)_2(CH_3OH)_2(H_2O)_2\cdot(CH_3OH)\}_n$ chains.

are similar to those of the dilute $[Gd_{0.98}Eu_{0.02}(H_2O)_4]_2(C_4O_4)_3$ compound in which europium emission quenching by the presumed (unidentified) traps at ca. 20 500 cm^{-1} are efficient. Further insight was sought from compounds **1** and **3**.

Luminescence Decay Dynamics of $Eu^{3+}(^5D_0)$ Emission in Crystals of the One-Dimensional Complex with $\{Eu(\mu\text{-}C_6H_5C_4O_3)_2(C_6H_5C_4O_3)_2(CH_3OH)_2(H_2O)_2\cdot(CH_3OH)_2\}_n$ Chains (1). The luminescence decay curves of Eu^{3+} following direct excitation of the $^5D_0$ level at 580 nm in the one-dimensional chain compound **1** are perfectly exponential for over five lifetimes and are temperature independent for $T < 220$ K; the corresponding spontaneous decay rate of the europium(III) $^5D_0$ emission is ca. 5.9×10^3 s^{-1}. For $T > 220$ K the decay curves are also perfectly single exponential, but they are temperature dependent, the corresponding thermal barrier being ca. 1.9×10^3 cm^{-1}. Introduction of inert Ln(III) ions such as La^{3+} does not affect the decay behavior significantly, but paramagnetic ones, namely, Sm^{3+} and Dy^{3+}, do quench the europium(III) $^5D_0$ emission in a manner approximating Stern−Volmer kinetics.[9] The decay curves remain perfectly exponential at 77 K throughout the concentration ranges $0 < x < 0.9$ for $\{Eu_{1-x}Ln_x(\mu\text{-}C_6H_5C_4O_3)_2(C_6H_5C_4O_3)_2(CH_3OH)_2(H_2O)_2\cdot(CH_3OH)\}_n$, Ln = Sm, Dy (Figure 7). Introduction of scatterers, such as La^{3+}, in mixed europium−dysprosium samples did not result in the large reductions in decay rates expected[5,6,10,11] for dominant one-dimensional energy transport regimes. For example, for $\{(Eu_{0.74}Dy_{0.26})(\mu\text{-}C_6H_5C_4O_3)_2(C_6H_5C_4O_3)_2(CH_3OH)_2(H_2O)_2\cdot(CH_3OH)\}_n$ and $\{(Eu_{0.77}La_{0.12}Dy_{0.11})(\mu\text{-}C_6H_5C_4O_3)_2(C_6H_5C_4O_3)_2(CH_3OH)_2(H_2O)_2\cdot(CH_3OH)\}_n$ the decay rates of $Eu^{3+}(^5D_0)$ emission were of similar magnitude, 6.4×10^3 and 5.9×10^3 s^{-1}, respectively. The energy transport regime is therefore predominantly multidimensional despite the large difference in the shortest intrachain (8.265 Å) and interchain (13.742 Å) Eu···Eu separations. This strongly suggests that Eu···Eu interactions are very strong and energy transport is in the dynamic regime.[10] The direct nearest neighbor Eu^{3+} to Ln^{3+} energy transfer rates obtained at 77 K for dilute samples $\{(Eu_{0.12}Ln_{0.88})(\mu\text{-}C_6H_5C_4O_3)_2(C_6H_5C_4O_3)_2(CH_3OH)_2(H_2O)_2\cdot(CH_3OH)\}_n$, 2.9×10^3 s^{-1} (Ln = Sm) and 2.7×10^3 s^{-1} (Ln = Dy), are similar to those estimated from the corresponding Stern−Volmer plots (3.4×10^3 and 3.1×10^3 s^{-1} for Ln = Sm and Dy, respectively). With the assumption that energy transfer is predominantly by dipole−dipole interactions and with application ofthe Förster−Dexter relationship[12] [$k(Eu-Ln) = C/R^n$], the dipolar coupling constants (C) responsible for the energy transfer at 297 K are weak, ca. 1×10^{-50} m^6 s^{-1} for both Eu−Sm and Eu−Dy couples, respectively. k(Eu−Ln) equals the direct energy transfer rate from $Eu^{3+}(^5D_0)$ to Ln^{3+}; R is the shortest Eu−Ln separation; and n denotes the order of the multipolar interaction, which is 6 for dipoles.

Luminescence Decay Dynamics of $Eu^{3+}(^5D_0)$ Emission in Crystalline Complex with Discrete Dimers $\{Eu[\mu\text{-}(C_6H_5)_2NC_4O_3]_2[(C_6H_5)_2NC_4O_3][NO_3][H_2O]_4\}_2\cdot 4H_2O$ (3). The luminescence decay of $Eu^{3+}(^5D_0)$ emission (excitation at 580 nm) in crystals containing small amounts of Eu^{3+} ions, $\{(Eu_{0.20}Gd_{0.80})[\mu\text{-}(C_6H_5)_2NC_4O_3]_2[(C_6H_5)_2NC_4O_3][NO_3][H_2O]_4\}_2\cdot 4H_2O$ **(4)**, are temperature independent for $T < 80$ K. The corresponding spontaneous decay rate extracted from the single-exponential curves is ca. 7.0×10^3 s^{-1}. For $T > 80$ K the temperature dependence is biphasic: for $80 < T < 200$ K, the thermal barrier to the quenching of the $Eu^{3+}(^5D_0)$ emission is a phonon of ca. 76 cm^{-1}, while that of $200 < T < 320$ K is ca. 2.0×10^3 cm^{-1}. On the other hand, the decay behavior of $Eu^{3+}(^5D_0)$ emission in the pure europium complex **3**, is temperature independent only up to 20 K, the spontaneous decay rate, 6.1×10^3 s^{-1}, being of similar magnitude to that of the dilute europium complex **4**. Luminescence from compound **3** features single-exponential decay behavior and a biphasic temperature dependence with thermal barriers of 64 and 2.2×10^3 cm^{-1} for $20 < T < 155$ and $155 < T < 230$ K, respectively, which again are very similar to those of the dilute complex, **4**. Emission of **3** is too weak to measure at $T > 230$ K. These results suggest that similar quenching mechanisms are active for both the dilute and pure europium complexes, but the population of accessible quenchers is much higher in **3** compared to those of **4**. For example, a comparison of the decay rates of dilute **4** and pure **3** europium(III) complexes at 220 K (9.3×10^3 and 9.1×10^4 s^{-1}, respectively) reveals much greater quenching of $Eu^{3+}(^5D_0)$ emission in **3**. Since the decay curves are perfectly single exponential for both the dilute Gd/Eu **4** and pure Eu/Eu **3** complexes and the thermal barriers are very similar, the results show that $Eu^{3+}-Eu^{3+}$ electronic interactions are strong.[1,2,4−6,11,13] Thus, many more active quenchers, which are common to both **3** and **4**, are encountered (via energy migration) in **3** than in **4**. As is the case for compounds **1** and **2**, energy migration on the Eu^{3+} sublattice in **3** is so efficient that energy transport is in the dynamic regime despite the relatively large differences in the closest intramolecular (6.264 Å) and intermolecular (9.201 Å) Eu···Eu separations. Furthermore, introduction of lanthanide(III) traps into the dimeric complex produces $\{(Eu_{1-x}Ln_x)_2[\mu\text{-}(C_6H_5)_2NC_4O_3]_2[(C_6H_5)_2NC_4O_3][NO_3][H_2O]_4\}_2\cdot 4H_2O$ (Ln = Sm, Dy) crystals in which quenching of $Eu^{3+}(^5D_0)$ emission yields perfectly single-exponential decay curves expected of a dynamic energy transport regime and approximate Stern−Volmer quenching kinetics. The direct 77 K Eu−Ln transfer rates (1.3×10^3 s^{-1} (Eu−Sm); 7.8×10^3 s^{-1} (Eu−Dy)) derived from corresponding Stern−Volmer plots are of the same order of magnitude as those obtained from decay curves of samples containing small amounts of Eu^{3+} ions, e.g. 1.3×10^3 s^{-1} for $\{(Eu_{0.02}Sm_{0.98})_2[\mu\text{-}C_6H_5)_2NC_4O_3]_2[(C_6H_5)_2NC_4O_3][NO_3][H_2O]_4\}_2\cdot 4H_2O$. Again with the assumption that the energy transfer is

(9) Stern, O.; Volmer, M. *Phys Z.* **1919**, *20*, 183.
(10) Huber, H. *Phys. Rev.* **1979**, *B20*, 2307, 5333.
(11) McPherson, G. L.; Waguespack, Y. Y.; Vanoy, T. C.; Rodriguez, W. J. *J. Chem. Phys.* **1990**, *92*, 1768.
(12) (a) Dexter, D. L. *J. Chem. Phys.* **1953**, *21*, 836. (b) Förster, T. Z. *Naturforch.* **1949**, *49*, 321.
(13) Howell, R. C.; Spence, K. V. N.; Kahwa, I. A.; White, A. J. P.; Williams, D. J. *J. Chem. Soc., Dalton. Trans.* **1996**, 961.

predominantly dipolar and with application of the Förster−Dexter relationship, the coupling constants responsible for the $Eu^{3+}(^5D_0)$ to Ln^{3+} energy transfer are 5×10^{-52} and 8×10^{-53} $m^6\ s^{-1}$ for Ln = Dy and Sm, respectively.

Conclusions

Europium−europium electronic interactions in complexes of europium(III) with squarate **2** and the monosubstituted squarate ligands, phenylsquarate **1**, and (diphenylamino)squarate **3** are very strong and multidimensional. As a result, the energy transport process in all the complex systems studied is in the dynamic regime irrespective of the structural dimensionality of the emitting metal ion array. The Eu(III)···Sm(III) and Eu(III)···Dy(III) electronic couplings are much weaker than those of Eu^{3+}···Eu^{3+}. Since energy migration efficiency is high in crystals dominated by dimeric, chain, and layer arrays of Eu^{3+} ions, the $Eu^{3+}(^5D_0)$···$Eu^{3+}(^5D_0)$ electronic interactions responsible for the migration process are largely through space rather than exchange. Taken together, the luminescence quenching dynamics of the dimeric (**3**), chain (**1**), and layer (**2**) compounds are unequivocal in indicating that thermalized quenching is predominantly by fast migration on the Eu^{3+} sublattice to traps. The excitation spectra of compounds **1** (Figure 5c; note the broad shoulder at 450−500 nm) and **3** (Figure 6a; note broad absorption at wavelengths > 460 nm) show broad low-energy absorption shoulders which may serve as traps for europium excitation. The luminescence quenching thermal barriers of ca. $(2.0-3.0) \times 10^3\ cm^{-1}\ mol^{-1}$ exhibited by compounds **1**−**3** are then the energies required for the requisite metal-to-ligand back-energy transfer. This argument is plausible for compound **1** for which introduction of inert Ln(III) ions such as La^{3+} does not affect the decay kinetics significantly. However, the quenching activity of such low-energy ligand states should not have to depend on energy migration as the decay dynamics of compounds **2** and **3** suggest (vide supra). The plausible explanation is, in this case, that a few active traps which are ca. $(2.0-3.0) \times 10^3\ cm^{-1}\ mol^{-1}$ above the emitting $Eu^{3+}(^5D_0)$ state are dispersed in the crystals and are accessible to $Eu^{3+}(^5D_0)$ excitons via rapid energy migration. However, such complicated thermalized $Eu^{3+}(^5D_0)$ emission quenching kinetics (with thermal barrier ca. $2 \times 10^3\ cm^{-1}$) can involve the $Eu^{3+}(^5D_1)$ state even though its exact role and the associated processes are not yet clear.[14] Indeed in one such case excitation of $Eu^{3+}(^5D_0)$ produced anti-Stokes $Eu^{3+}(^5D_1)$ emission.[14b] Given the prominent differences in the excitation spectra of **1**−**3**, common $Eu^{3+}(^5D_0)$ to $Eu^{3+}(^5D_1)$ internal conversion may indeed be the important rate-limiting step instead of some direct $Eu^{3+}(^5D_0)$-to-organic-type-trap energy transfer.

Acknowledgment. L.A.H. wishes to thank the St. Augustine Campus Committee on Graduate Studies, The University of the West Indies, for financial support. I.A.K. wishes to thank the InterAmerican Development Bank-UWI development program for the funds used to purchase the cryogenic equipment (R&D Project No. 29).

Supporting Information Available: X-ray crystallographic files, in CIF format, containing data for the structures of **1** and **3a**−**c** and Table S1 showing luminescence decay rates for pure and doped samples of **1**−**3**. This material is available free of charge via the Internet at http://pubs.acs.org.

IC9907664

(14) (a) Matthews, K. D.; Bailey-Folkes, S. A.; Kahwa, I. A.; McPherson, G. L.; O'Mahoney C. A.; Ley, S. V.; Williams, D. J.; Groombridge, C. J.; O'Connor, C. A. *J. Phys. Chem.* **1992**, *96*, 7021. (b) Kropp, J. L.; Dawson, W. R. *J. Chem. Phys.* **1966**, *45*, 2419. (c) Holtz, R. C.; Meister G. E.; Horrocks W. de W., Jr. *Inorg. Chem.* **1990**, *29*, 5183.